

# SHELL CRACKING IN INVESTMENT CASTING WITH LASER STEREOLITHOGRAPHY PATTERNS

W. L. Yao

Department of Mechanical and Production  
Engineering  
National Kaohsiung First University of Science  
and Technology  
Kaohsiung, Taiwan, R.O.C.

Ming C. Leu<sup>1</sup>

Department of Mechanical Engineering  
Multi-lifecycle Engineering Research Center  
New Jersey Institute of Technology  
Newark, New Jersey 07102

## ABSTRACT

This paper presents an investigation of ceramic shell cracking during the burnout process in investment casting with internally webbed laser stereolithography patterns. We hypothesize that shell cracking will occur when the rupture temperature of the ceramic shell is lower than both the glass transition temperature of the pattern material and the web link buckling temperature. The hypothesis is validated by our experimental observations which confirm the numerical predictions from our finite element analysis. This provides a basis for design of the internal web geometry of a lithography pattern and evaluation of the burnout process with such a pattern. We show the shell cracking and web link buckling temperatures to be functions of the pattern geometry (including the cross-sectional dimensions and span length of the web link) and the shell thickness.

*Keywords:* Rapid Prototyping; Investment Casting; Solid Freeform Fabrication; Rapid Tooling;

## 1. INTRODUCTION

Investment casting is a precision casting process. It begins with the making of an expendable pattern – usually produced by injection of liquid wax into a precision mold. The wax pattern is assembled with gating and feeding subsystems and cleaned prior to the ceramic coating. The coating is built through successive stages of dipping and stuccoing. This procedure is repeated until the required shell thickness is obtained. On completion of the coating the expendable wax pattern is removed by melting in a steam autoclave or flash furnace, and the ceramic shell is fired prior to casting. After the molten metal is poured and solidified, the shell is broken away and the castings removed [1].

Solid freeform fabrication (SFF) is increasingly being used for tooling and manufacturing applications, besides making design prototypes from CAD models. The use of Stereolithography Apparatus (SLA) is the most popular among the various SFF technologies existing today. SLA builds a part by controlling a laser beam to selectively cure photocurable liquid resin layer by layer [2] [3] [4] [6]. The SLA built epoxy pattern can be used as a thermally expendable pattern

---

<sup>1</sup> Dr. Ming C. Leu is on leave at the National Science Foundation as the Program Director for Manufacturing Machines and Equipment.

in investment casting. Compared with the conventional wax pattern, this enables prototyping new physical products more quickly and cost effectively. However, because the coefficient of thermal expansion of the epoxy resin is one order of magnitude larger than that of investment ceramic material, the ceramic shell may crack during the pattern burnout process. Cracking occurs when the stress induced in the ceramic shell is greater than the Modulus Of Rupture (MOR) of the shell material.

There have been some studies about thermal effects on the webbed pattern and ceramic shell in investment casting, but the generated knowledge is still very limited [5] [7] [8] [9] [10]. A research team at 3D Systems, the SLA manufacturer, developed quasi-hollow webbed patterns in investment casting (see Figure 1) Jacobs [7] observed the yield of castings as a function of the pattern void ratio, defined as the fraction of air space in a pattern. He stated that under such a situation the SL webbed pattern will collapse inwards under the influence of heat, rather than cracking the ceramic shell by expanding outwards. Hague and Dickens [8][9] observed shell cracking at temperatures below the glass transition temperature of the epoxy material, but did not observe buckling of hollow SL patterns in their burnout experiments.

The objective of this study is to provide a better understanding about why quasi-hollowed SL models cause cracking in the ceramic shells and what causes the webbed pattern to collapse. Our hypothesis is that shell cracking will occur when the temperature of shell rupture is lower than the glass transition temperature of epoxy resin and the temperature of web buckling. This hypothesis is verified by our experimental observations which confirm that the cracking of the shell can be prevented if either the material softens or the web links buckle during the burnout process. An analytical model with finite element analysis is used to determine the stresses in the webbed pattern and the ceramic shell during the burnout process.

## 2. HYPOTHESIS DESCRIPTION

When an investment casting shell with an SL epoxy pattern inside is placed in an autoclave or flash-fire oven during the burnout process, it is subjected to high temperature rise, thermal expansion, and large strains. Since the difference between the coefficient of thermal expansion of pattern material (epoxy) and that of investment material (ceramic) is more than one order of magnitude, the epoxy pattern exerts considerable stresses on the ceramic shell. Under the influence of heat, whether an investment shell will break or not depends upon factors governed by the epoxy web structure and the investment shell. The primary hypothesis of this work is the follows: whether the shell cracking, pattern buckling, and epoxy softening occurs first depends on which of the pattern buckling temperature ( $T_b$ ), the resin glass transition temperature ( $T_g$ ), and the shell rupture temperature ( $T_u$ ) is the lowest. If the epoxy resin softens or the internal epoxy web structure buckles first, the exerted stress upon the shell wall will drop dramatically, thus keeping the shell intact. On the other hand, the cracking of the ceramic shell will occur if the shell rupture temperature is lower than both the pattern buckling temperature and the resin glass transition temperature.  $T_u$  is the temperature at which the induced stress is greater than the MOR of the shell ceramic material;  $MOR = S_u = 3.0\text{MPa}$  in this study [13].  $T_g$  is the glass transition temperature of the epoxy resin,  $T_g = 60 - 70^\circ\text{C}$  for SL5170 epoxy from Ciba-Geigy [8] [9].  $T_b$  is the temperature at which the compressive pressure causes the web link to

buckle. The temperatures of shell cracking and web link buckling are related to the dimensions of the web structure and the thickness of the investment ceramic shell.

### 3. FINITE ELEMENT ANALYSIS

Since the skin of SL pattern is very thin, the effect of the outer skin can be negligible in the analysis. The internal square web structure pattern can be treated as a girder-type planar frame with fixed ends (see Figure 2). Due to the complexity of the internal web structure, it is necessary to perform numerical simulations to determine stresses induced in the burnout process. In this analysis, a two-dimensional model of a ceramic shell with the internal web structure, under a heating process to stepwise isothermal temperatures, is assumed. The buckling of a square frame is adopted to determine the temperature of web structure buckling. To simplify the analysis, we do not consider transient heat transfer during the thermal expansion of the pattern and shell. The basis of the two-dimensional model is the “simple, topologically connected” internal web structure, i.e. two consecutive layers of the internal web structure are simply stacked without any interaction in the z-direction (see Figure 1). Additionally, the temperature uniformity within the webbed pattern and the ceramic shell is assumed throughout this study. Practically it is difficult to keep the temperature uniform during the burnout process of the specimens. For each step temperature increase, the oven temperature is increased and kept long enough to reach the desired temperature. The assumption on the buckling of the internal web structure is based on the confluence of a number of small square grids in the webbed pattern and the rigidity of the joints of the internal web structure to preserve the angles between the various link members [11]. Due to the thermal expansion, the resultant forces are likely to cause the individual square grids to buckle (see Figure 3). Our experimental observations (to be discussed) show a good agreement with the FEA results with the model of square frame buckling. The previous use of the buckling of a beam with two fixed ends was less accurate [12]. The square frame buckling model enables determining the buckling temperature of the web link structure.

The numerical result of a part ( $L=6.35\text{mm}$ ,  $b=0.3048\text{mm}$ , and  $h=1.4372\text{mm}$ ) with 1mm thickness ceramic shell is depicted in Figure 4. The FEA models used in this study are quarter models and they are automatically meshed in level #2 using the PLANE82 element and axisymmetric boundary condition. The  $\sigma_c$  and  $\sigma_x$  (or  $\sigma_y$ ) represent the principal (hoop) stress in the ceramic shell and the compressive stress in the epoxy webbed pattern, respectively. The  $\sigma_c$  value is compared with MOR to define the rupture temperature of the ceramic shell.  $P_{cr}$  is the critical pressure that causes the web link to buckle. The critical unit pressure of the buckling of square frame,  $P_{cr}$  is  $16.47EI/AL^2$  [11], where  $A$  is the cross-sectional area of web link,  $E$  is Young's modulus of the epoxy material,  $I$  is the moment of inertia of web link cross-section, and  $L$  is the web link space length.  $A = b \times h$  and  $I = hb^3/12$ , where  $b$  is the width of web structure, and  $h$  is the depth of web structure. This  $\sigma_x$  value is compared with  $P_{cr}$  to determine the buckling temperature of the web link. For this part the obtained results are  $T_u = 35^\circ\text{C}$ , and  $T_b = 52^\circ\text{C}$  (refer to Table 1). Note that Young's modulus of the epoxy resin is a function of temperature. Figure 5 shows the effects of the ceramic shell thickness on the generated stresses in the ceramic shell and webbed pattern. It is seen from Figure 5a that the maximum hoop stress decreases as the shell thickness is increased. That is, a thicker ceramic shell can better resist the thermal expansion of the SL epoxy pattern. Figure 5b shows that the shell thickness effect on the maximum

compressive stress in the internal web structure is quite small. In fact, the stress curves for 6mm and 9mm thickness are indiscernible.

#### **4. EXPERIMENTAL STUDY**

The experimental study consists of two parts. First, experiments are conducted to observe the pattern burnout process. Figure 6 shows an SL pattern without and with the ceramic shell. Second, the induced stresses on the shell are measured by strain gauges. Figure 7 shows strain gauged samples. Both the qualitative observations and the strain gauge measurements validate the prediction of FEA.

The test samples are geometrically designed with the Pro/ENGINEER package and built using SLA250 with the SL5170 epoxy resin from Ciba-Geigy. The internally webbed SL samples have a simple cylindrical geometry of 25.4mm (1inch) diameter and 76.2mm (3inch) long. The built parts are coated with ceramic using a Sandia National Laboratories facility.

A number of experiments have been carried out to observe the pattern burnout process. The oven used for the experiments has its temperature controlled electrically. The test samples are examined and recorded at the interval of ten degrees, up to 100°C. The observations of test samples are made with a magnifier and an imaging camera. The observations recorded include shell cracking, epoxy softening, and web link buckling. For the test samples with strain gauges, the pattern is coated with ceramic slurry after mounting the strain gauges on the surface of each pattern. If the webbed SLA pattern collapses because of the buckling of the web structure, the web link will look wavy. If the pattern collapses because of epoxy resin softening, then the pattern will look “leathery”.

#### **5. RESULTS AND DISCUSSION**

Several phenomena of the pattern burnout process have been observed. These observed phenomena include 1)shell cracked, 2)web link slightly buckled, 3)web link severely bucked, 4)no buckling in the web link, and 5)web link buckled and shell cracked. The basic test sample has the typical dimensions of web structure ( $L=6.35\text{mm}$ ,  $b=0.3048\text{mm}$ , and  $h=1.4732\text{mm}$ ) used in the QuickCast build process. The samples of this part that are invested with 1mm shell thickness show shell cracking when the temperature reaches 40°C. This is shown in Figure 8a. The web links remain straight because the shell has cracked already. This observation indicates that the shell cracking occurs at early stages of the burnout process in investment casting, when the invested shell is not strong enough to resist the exerted forces from the thermal expansion of the internal web structure. From FEA, the predicted rupture temperature is about 35°C (see Figure 5), at which the induced stress exceeds the MOR of the ceramic material and thus fractural cracking occurs.

The observations show that the web links of the basic test samples (with the typical web structure) and 3, 6, 9mm in shell thickness are slightly buckled when the temperature reaches 50°C. There is no occurrence of shell cracking at all, whereas the web link becomes brittle and collapsed after the glass transient temperature. Likewise, the web links of the test samples with a

smaller web link height and coated with 6 and 9mm thickness appears slightly buckled. Again, the results of FEA are confirmed by the experimental observations.

The experimental results of the test samples which have 50% longer web link span than the basic test samples and coated with 6mm and 9mm ceramic, show that the web link becomes very wavy when the temperature reaches around 40°C (see Figure 8b). The temperature (37°C) at which the web link starts to bend is significantly lower than the glass transition temperature (60 - 70°C) of the epoxy material. The test samples which have a web span length smaller than the typical web structure by 50% and coated with 6mm and 9mm ceramic show that the web structure becomes brittle and breaks down at high temperatures (> 100°C) with no sign of web link bending (see Figure 8c). The buckling temperature of this part is infinity, which means that buckling will never occur. The experimental observations of test samples which have 50% longer web link span than the basic test samples and coated with 1mm ceramic show that the web links buckle but the ceramic shell still cracks. The FEA results predict that for this part, the web link buckles and the shell cracks at about the same low temperatures. The experimental observations confirm the FEA predictions for the relationships among  $T_b$ ,  $T_g$ , and  $T_u$  for all these test parts.

An example of experimentally measured stresses on the strain gauged test samples is shown in Figure 9. The experimental data exhibit the same trend as the predictions from the finite element analysis. The discrepancy between the predicted and measured results is due primarily to the following: 1)The material property of the thermoset epoxy resin is uncertain after the glass transition temperature (60 - 70°C), which makes numerical predictions difficult at temperatures near and above 60°C. 2)Our FEA assumes constant temperature of the shell-pattern construction during the burnout process and does not take transient heat transfer into consideration. Although the oven temperature is kept constant for a period of six minutes after heating up for each interval of ten degrees, the temperature of the shell-pattern construction is still not uniform and cannot be simply represented by the measured temperature at the center of the webbed structure. A longer duration will be needed in future experiments, or a transient heat transfer model needs to be developed.

## 6. CONCLUSION

The mechanisms of shell cracking and internal web structure collapse are clarified by the described numerical and experimental study of investment casting with internally webbed stereolithography pattern. Finite element analysis shows that the shell cracking and web link buckling temperatures are functions of the pattern geometry (including the cross-sectional dimensions and the span length of the web link) and the shell thickness. The pattern with a longer web span and a smaller moment of inertia buckles more readily under the influence of heat. The experimental observations agree fairly well with the numerical predictions both qualitatively and quantitatively. Thus the shell cracking can be prevented by the buckling of epoxy webbed pattern in early stages of the burnout process. Simulation of the burnout process and evaluation of a new internal web structure design can be made by the described approach.

## ACKNOWLEDGMENT

This work was partially supported by the Multi-lifecycle Engineering Research Center at New Jersey Institute of Technology and by the National Science Foundation. The coating of ceramic on the test parts was done with the help of Michael Maguire at Sandia National Laboratories. We are also thankful to the Center for Manufacturing Systems and Center for Environmental Engineering and Science at New Jersey Institute of Technology for their help and cooperation.

## REFERENCES

1. Kalpakjian, S. *Manufacturing Processes for Engineering Materials*, Chapter 5, 1991.
2. Conley, J. G., and Marcus, H. L., "Rapid Prototyping and Solid Free Form Fabrication," *Journal of Manufacturing Science and Engineering, ASME*, 1997, Vol. 119, pp 811 - 816.
3. Koch, M., "Rapid Prototyping & Casting," *3rd European Conference on Rapid Prototyping & Manufacturing*, 1994.
4. Sachs, E., et al., "Micro-Constructive Manufacturing by 3D Printing," *Proc. Of the 1994 NSF Design and Manufacturing Grantees Conference, Cambridge, MA*, 1994.
5. Blake, P., Baumgardner, O., Haburay, L., and Jacobs, P., "Creating Complex Precision Metal Parts Using QuickCast," *Proceedings of SME Conference on Rapid Prototyping & Manufacturing*, April, 1994.
6. Jacobs, P., *Rapid Prototyping and Manufacturing Fundamentals of Stereolithography*, SME, Dearborn, MI, 1992.
7. Jacobs, P., "QuickCast 1.1 & Rapid Tooling," *NASUG 1995 Annual Meeting and Conference*, Tampa, FL, 1995.
8. Hague, R., and Dickens, P. M., "Stresses created in ceramic shells using QuickCast models," *First National Conference on Rapid Prototyping and Tooling Research*, Buckinghamshire College, UK, 1995, pp. 89-100.
9. Hague, R., and Dickens, P. M., "Requirements for the successful autoclaving of stereolithography models in the investment casting process," *Second National Conference on Rapid Prototyping and Tooling Research*, Buckinghamshire College, UK, 1996, pp. 77-92.
10. Pang, T. H., "Advances in Stereolithography Photopolymer Systems," *Stereolithography and other RP&M Technologies*, SME Dearborn, MI, July 1996, Chapter 2.
11. Wang, C. T., *Applied Elasticity*, McGraw-Hill, New York, 1953, Chapter 9, pp. 209-239.
12. Yao, W. L., Wong, H., Leu, M. C., and Sebastian, D. H., "An Analytic Study of Investment Casting with Webbed Epoxy Patterns," *Proceedings of ASME 1996 Winter Annual Conference and Rapid Response Manufacturing (RRM) Symposium*, Atlanta, GA, 1996, MED-Vol. 4, pp. 11-15.
13. Sandia National Laboratories, *Properties of Investment Ceramic*, 1995.

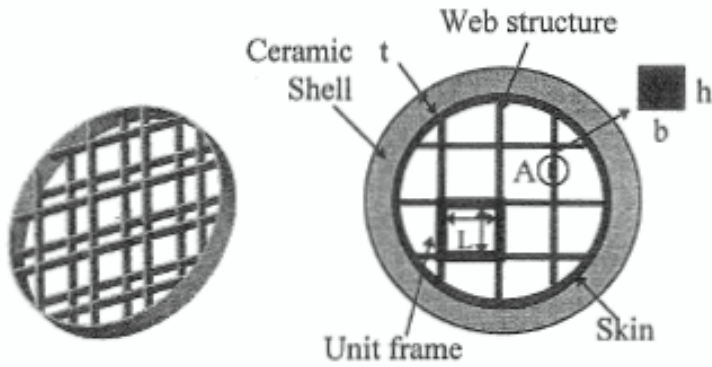


Figure 1 Typical offset layers of web structure in SL quasi-hollow pattern.

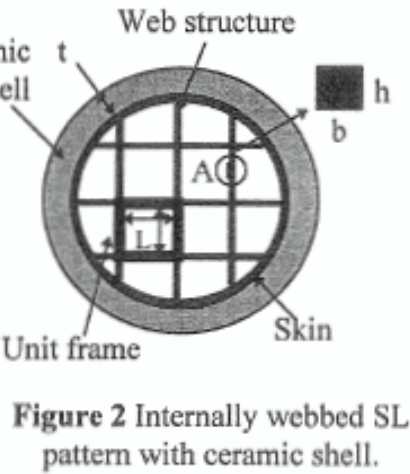


Figure 2 Internally webbed SL pattern with ceramic shell.

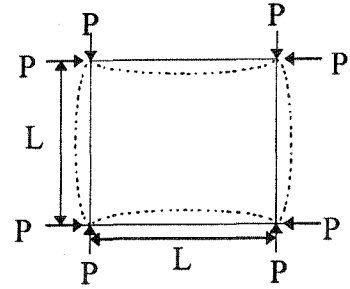


Figure 3 The buckling of square frame under compressive loads.

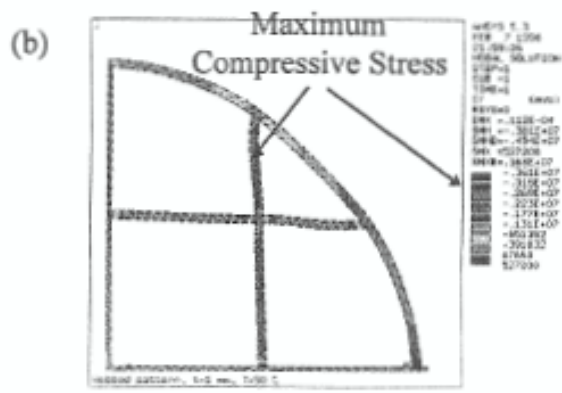


Figure 4 The stress profile from the FEA result for Part1 with 1mm ceramic shell: (a) hoop stress in ceramic shell and (b) compressive stress in webbed pattern.

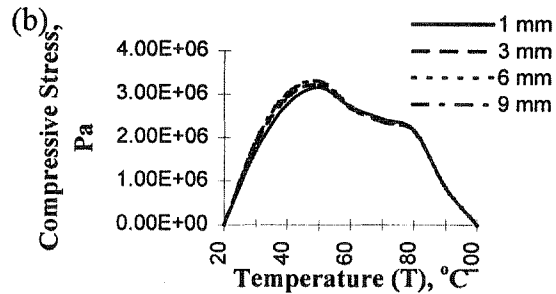
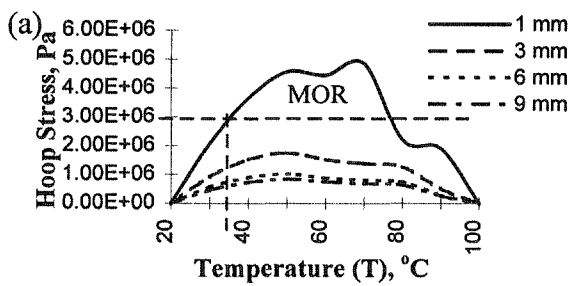


Figure 5 Stresses varied with temperature for different shell thickness: (a) maximum hoop stress in the ceramic shell and (b) maximum compressive stress in the webbed pattern.

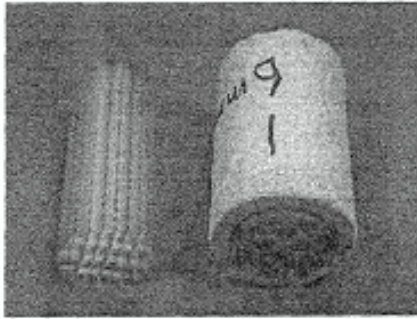


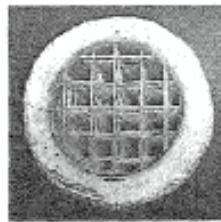
Figure 6 SL pattern without and with ceramic shell.



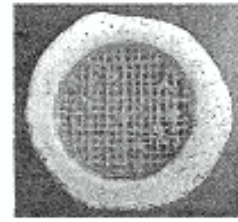
Figure 7 Samples mounted with strain gauges in a temperature controlled oven.



(a)



(b)



(c)

Figure 8 Several observed phenomena of the pattern burnout process: (a) shell cracked, (b) web links bend severely, and (c) web link do not bend.

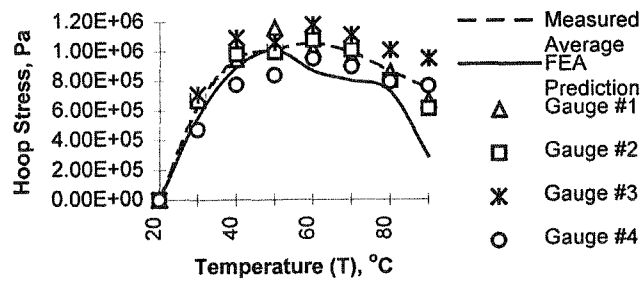


Figure 9 Comparison of measured and prediction hoop stress at the shell-pattern interface.

Table 1 Comparison of analytical values of  $\sigma_c$  and  $\sigma_x$  with MOR and  $P_{cr}$ , respectively, to determine  $T_u \approx 40^\circ\text{C}$  and  $T_b \approx 50^\circ\text{C}$ .

T (°C)	$\sigma_c$ (Pa)	$\sigma_x$ (Pa)	$P_{cr}$ (Pa)
30	$2.07 \times 10^6$	$1.69 \times 10^6$	$6.30 \times 10^6$
40	$3.64 \times 10^6$	$2.76 \times 10^6$	$5.20 \times 10^6$
50	$4.55 \times 10^6$	$3.15 \times 10^6$	$3.24 \times 10^6$
60	$4.43 \times 10^6$	$2.71 \times 10^6$	$0.28 \times 10^6$